# Drag reduction by applying speedstrips on rowing oars

Kuyt, C.B.; Greidanus, A. J.; Westerweel, J.

**DOI**
10.1016/j.proeng.2016.06.198

**Publication date**
2016

**Document Version**
Final published version

**Published in**
Proceedings of 11th Conference of the International Sports Engineering Association, ISEA 2016

**Citation (APA)**
Kuyt, C. B., Greidanus, A. J., & Westerweel, J. (2016). Drag reduction by applying speedstrips on rowing oars. In A. J. Jansen (Ed.), *Proceedings of 11th Conference of the International Sports Engineering Association, ISEA 2016: The Engineering of SPORT 11* (pp. 110-115). (Procedia Engineering; Vol. 147). Elsevier. https://doi.org/10.1016/j.proeng.2016.06.198

Available online at www.sciencedirect.com

ScienceDirect

Procedia Engineering 147 (2016) 110 – 115

Procedia Engineering

www.elsevier.com/locate/procedia

11th conference of the International Sports Engineering Association, ISEA 2016

# Drag reduction by applying speedstrips on rowing oars

C.B. Kuyt, A.J. Greidanus*, J. Westerweel

*Delft University of Technology, Mekelweg 2, 2628 CD Delft, Netherlands*

**Abstract**

The objective of this study was to determine the advantage of the application of speedstrips to rowing oars for a lightweight single sculler. The research method comprehended three steps: (1) the analysis of the rowing oar movement, (2) the determination of the change in drag and (3) the composition of a rowing model to establish the advantage that could be achieved. The parameters needed for the model: boat velocity, oar angle velocity and power delivered by the rower, were recorded on a real single sculler. The change in drag due to speedstrips on cylinders was determined by performing wind tunnel experiments. The rowing model (Matlab) simulates a race by using real stroke data of a world-class rower as input, while calculating the drag with the coefficients determined by the wind tunnel experiments. The output of the model is the final advantage by the application of speedstrips to rowing oars. Speedstrips induce a 0.1% advantage over a 2000 m race under calm wind conditions. The advantage increases up to 0.4% with a headwind velocity of 5 m $s^{-1}$. For bigger boats, the advantage could be even more significant.

Peer-review under responsibility of the organizing committee of ISEA 2016

*Keywords:* rowing; aerodynamics; speedstrips; zig-zag strips; artificial boundary layer transition; rowing model;

## 1. Introduction

The goal in rowing is to cover a distance (e.g. 2000 m) as fast as possible. This is achieved by maximizing propulsion and minimizing drag. This study focusses on the minimization of the aerodynamic drag on the rowing oars by the use of zig-zag strips. Zig-zag strips have been successfully applied in sports before. Dutch speed-skaters used zig-zag strips on their heads during the Nagano Winter Olympics 1998 to reduce air-resistance and won 11 medals (5 Gold). Since 2000 these ‘speedstrips’ have also been used in rowing to reduce the air-resistance of rowing oars, even though this air-resistance is very small compared to the total resistance a rowing boat encounters during forward motion [1]. Athletes and coaches have always been sceptical of the magnitude of this advantage.

The goal of this study is to quantify the advantage of speedstrips applied to the rowing oars of a lightweight single scull. First, the theoretical background is explained in Section 2. In Section 3, two experiments are outlined as well as the model that simulates the rowing mechanism and quantifies the advantages. The results of the experiments and the simulation are presented in Section 4. The overall conclusions of this research are given in Section 5.

* Corresponding author. Tel.: +31152784194
*E-mail address:* a.j.greidanus@tudelft.nl

1877-7058 
Peer-review under responsibility of the organizing committee of ISEA 2016
doi:10.1016/j.proeng.2016.06.198

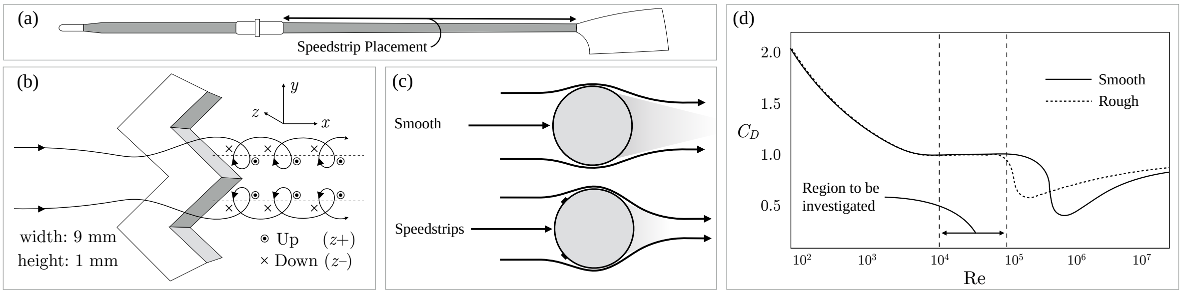


Fig. 1: (a) Speedstrip placement; (b) Flow over speedstrip; (c) Cylinder flow and wake; (d) Cylinder drag coefficient $C_D$.

## 2. Theoretical background of speedstrips on rowing oars

The shaft of a rowing oar is considered to be cylindrical. The air flows around the oar shaft and results in a wake behind the oar. The size of the wake is a measure of the drag on the cylinder; the larger the wake, the larger the drag (Fig.1(c)). The aerodynamic drag of a cylindrical oar shaft is given by $F_D = \frac{1}{2}\rho V^2 C_D A$ (1), where $\rho$ is the air density, $V$ is the air flow velocity relative to the oar, $C_D$ is the drag coefficient and $A$ the frontal area. The drag coefficient $C_D$ is a function of the Reynolds number *Re*, which is given by $Re = VD/\nu$ (2), with $D$ the cylinder diameter and $\nu$ the kinematic viscosity of air[2]. Empirical data for the $C_D$-*Re* curve for cylinders is found in literature [3,4], including data for smooth and rough cylinder surfaces (Fig.1(d)). A rough cylinder surface shows an earlier transition to the so-called 'drag crisis', which is a sudden drop in $C_D$ value, compared to the smooth cylinder surface. The critical Reynolds number for rough cylinder surfaces is achieved around $Re \sim 5 \cdot 10^4$. The surface roughness initiates instability which causes turbulence in the boundary layer and results in reattachment of the flow onto the surface [4]. The delay of the flow separation decreases the size of the wake, which is primarily responsible for the pressure difference between the front and the back of the cylinder (i.e. drag). Aoki et al. [5] and Choi et al. [6] have shown that the same phenomenon occurs for dimples in golf balls.

The Reynolds number regime of the flow around an oar shaft during rowing can be roughly estimated. The velocity of the air flow $V$ over the shafts in calm weather conditions is the superimposition of the boat velocity (5 m s$^{-1}$) and the oar velocity relative to the boat (0-5 m s$^{-1}$). The diameter of the shafts is between 3 and 5 cm. The oar shaft *Re*-regime is estimated to be around $10^4 < Re < 4 \cdot 10^4$, which is lower than the critical Reynolds number for a rough cylinder surface and makes a rough surface insufficient to reduce the drag of a rowing oar.

Forced turbulent boundary layer transition is also achieved by speedstrips. Surface roughness creates turbulence more randomly, while speedstrips create streak-like structures behind the speedstrips [7,8]. The speedstrip initiates counter-rotating vortices in the flow, as can be seen in Fig. 1(b). Within a specific Reynolds number range, speedstrips cause the turbulent boundary layer to separate later from the cylinder surface, and therefore decreasing the size of the wake (Fig.1(c)) and with that the aerodynamic drag. In rowing, speedstrips are placed on the oar shafts as shown in Fig. 1(a). The speedstrips have a $60^o$-zigzag geometry with a width of 9 mm and thickness of 1 mm (Fig. 1(b)). In this study, empirical drag data of speedstrips on a cylinder surface is obtained by wind tunnel measurements to determine the drag reducing ability of speedstrips on rowing oars.

## 3. Methodology and experimental procedure

The goal of this study is to quantify the advantage of applying speedstrips on oar shafts. The advantage is an increase in boat velocity due to a decrease in aerodynamic drag of the oar shafts. In this reserach, experiment 1 determines the Reynolds numbers of a rowing stroke as a function of time and oar geometry. Experiment 2 delivers the $C_D$-*Re* curve as a function of the Reynolds numbers for cylinders without and with speedstrips. As explained in the previous section, speedstrips are expected to induce a drag crisis for $Re < 5 \cdot 10^4$. Finally, a Matlab-model relates the drag reduction to an increase in boat velocity, which is translated into an advantage for a single sculler in a race relative to the case where speedstrips were not applied.

The decrease in power that is lost to drag can also be seen as an increase in power that is delivered to the system by the rower, as the energy balance is the same in both cases. Therefore, the delivered power by the rower in the direction of motion will be measured during experiment 1 to establish the relationship between power input and resulting velocity output. The velocity increase is translated to a length-advantage at the finish of a 2000 m race, to illustrate to the obtained result.

### 3.1. Experiment 1: Oar movement analysis

The rowing stroke of a single sculler has been analysed to obtain the required parameters: boat velocity ($V_{\text{boat}}$), oar angle ($\phi$), angular velocity ($\omega$) and the power delivered by the rower in the direction of motion ($P_y$), as shown in Fig. 2(a). The measurements were performed on a world-class under 23 lightweight rower in a single scull [11], by using an oarlock measurement device with a sampling frequency of 1 kHz [12]. The dimensions of the oars in the experiment and the simulation are identical; outboard shaft length $L_{\text{oar}} = 1.42$ m (between oarlock and blade), with a maximum thickness at the oarlock $D_{\text{max}} = 40$ mm and a minimum thickness $D_{\text{min}} = 35$ mm at the blade.

### 3.2. Experiment 2: Wind tunnel experiment

The goal of the wind tunnel experiment was to obtain the $C_D$-$Re$ curve for cylinders with speedstrips. An open wind tunnel facility was used for the experiments, with the experimental configuration shown in Fig. 2(c), (d) and (e). A cylinder was placed in front of the exhaust of the wind tunnel, attached to a stiff construction which kept it in place. Load cells measured the horizontal loads resulting from the airflow over the cylinder [13]. The drag force $F_D$ measured by the load cells (indicated as the bold vector in Fig.2(c)), is the variable used to calculate $C_D$ using equation (**??**). This variable depends on the air velocity $V$ (indicated as the thin vectors Fig.2(c)), which was controlled in the wind tunnel. The frontal area of the cylinder was estimated by using the diameter $D$ and length $L$ of the cylinder, $A = D \times L$. All other variables were assumed to be constant during every experiment. The experiment was carried out for multiple configurations, namely: varying cylinder diameter (32, 40 and 50 mm), varying surface roughness ($\varepsilon/d \approx 0$ for smooth, and 0.02 for rough) to validate the experimental method, with and without speedstrips (not for rough cylinders) and varying angle (0, 30 and 60 degrees) as is shown in Fig. 2(e) to verify assumptions in the model, which is explained in the next subsection.

### 3.3. Rowing model

The required parameters are obtained by experiment 1, containing the boat velocity $V_{\text{boat}}$, oar angle $\phi$, angular velocity $\omega$ and the power delivered by the rower in the direction of motion $P_y$ for every time step $t$. The oar shaft is divided in 100 segments of equal length to obtain the length at every location $r$. The parameters $V_{\text{boat}}$ and $\omega$ will be used to calculate the velocity at every location along the length of the oar shaft $r$ for every time step $t$. As can be seen

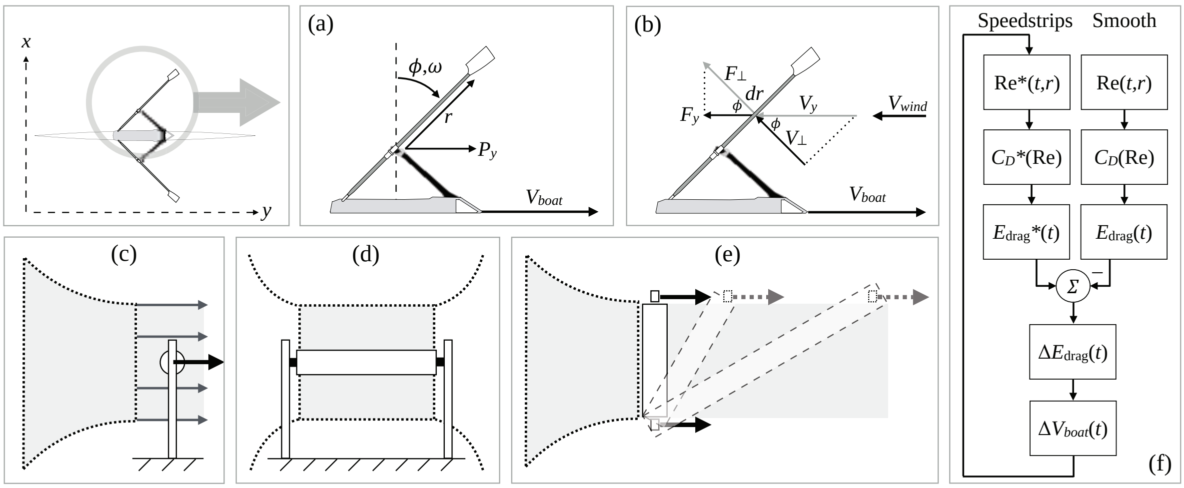


Fig. 2: Experiment 1: (a) Oar movement parameters; (b) Decomposition of velocities and forces. Experiment 2: experimental configuration (c) Side view; (d) Front view; (e) Top view. (f) Rowing model iteration process.

in Fig. 2(b), the wind velocity and the oar velocity have different directions. The model decomposes the velocity into components to obtain the flow velocity perpendicular to the oar by: $V_\perp = \cos(\phi)(V_{\text{wind}} + V_{\text{boat}}) - \omega r$. The velocity can be used to calculate the Reynolds number at every time step $t$ by equation (**??**). The diameter along the length of the oar shaft is not constant, but decreases outwards to the blade of the oar by: $D(r) = r(D_{\min} - D_{\max})/L_{\text{oar}} + D_{\max}$. Note that $D = D_{\max}$ at the oarlock ($r = 0$), and $D = D_{\min}$ at the blade ($r = L_{\text{oar}}$). The result of this data processing is a vector for one stroke cycle containing the Reynolds number as a function of time and location on the oar shaft: $Re(t, r)$, based on the perpendicular flow. The results for perpendicular flow obtained by experiment 2 are used to calculate the drag force acting on the oar, assuming quasi-steady flow conditions. The decomposition of the airflow gives accurate results for the drag force calculation, as it has been verified by measurements with cylinders under an angle (Fig.2(e)).

The drag force is calculated using equation (**??**). By using the perpendicular velocity $V_\perp$, the force will be in the same direction, as shown in Fig. 2(b). However, the drag force acting in the $y$-direction only influences the boat velocity. Therefore, the perpendicular drag force is decomposed into a force in the direction of the boat velocity: $F_y = \cos(\phi)F_\perp$. When the force at each $(r, t)$ is known, the velocity at every location $r$ multiplied by the force results in the corresponding energy loss. The energy loss to drag is calculated as follows: $E_{\text{drag}}(t) = F_{r,y}(t)V_{r,y}(t)$. When performing these steps for both an oar shaft with and without speedstrips, a difference in energy loss is obtained: $\Delta E_{\text{drag}}$. The energy difference $\Delta E_{\text{drag}}$ is used to re-calculate the boat velocity for the boat equipped with speedstrips. In physics, the law of energy conservation states that the total energy of an isolated system remains constant. The kinetic energy of the system increases when the energy loss to drag is reduced by the speedstrips.

Van Holst [9] has composed a rowing model that simulates the mechanics of rowing boat propulsion, and represents very accurate the propulsion and velocity of rowing boats in practice. The model relates the power input of the system to boat velocity as: $P_y = C_t V_{boat}^3$, where $C_t$ represents the total drag coefficient of the system. Using the delivered power $P_y$ and boat velocity $V_{boat}$ measured in experiment 1, an average total drag coefficient $C_t$ can be calculated. In this study, the $P$-$V$ relation is used in the composed rowing mechanics model to relate the energy saving due to speedstrips to an increase in boat velocity, rewritten as follows: $\Delta V_{boat} = \sqrt[3]{{V_{boat}}^3 + \Delta E/C_t} - V_{boat}$ (3). As a result, the increase in boat velocity induces an increase in the Reynolds numbers for a speedstrip-equipped boat. Therefore, the Reynolds numbers are updated every timestep $t$. The velocity increase multiplied by time results in a length advantage due to the application of speedstrips. During the simulation, the stroke is repeated until a length of 2000 m has been covered. The length advantage at the end of the race distance is the final result of the model. Fig. 2(f) shows a summary of this iterative calculation process. Furthermore, the simulation is carried out for different head wind velocities; an increase in headwind velocity will decrease the boat velocity. This is accounted for, by comparing weather data from the KNMI on Schiphol Airport [10] with race results of different races with the same crews on the "Bosbaan" rowing course next to the airport [14].

## 4. Results and discussion

### 4.1. Experiment 1

The rowing oar movement measurements have resulted in stroke data for processing. An example of a single stroke in race pace from this dataset is given in Fig. 3. The curves have been smoothed for clarity. The oar angle is not shown as it has only been used to obtain a complete stroke from beginning to end by verifying the oar location. The oar

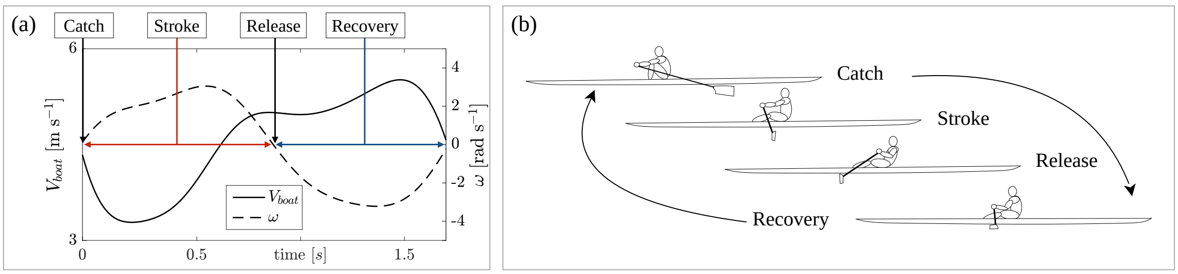


Fig. 3: (a) Single stroke from dataset of experiment 1. (b) Visualisation of stroke cycle.

angular velocity is shown only for the starboard oar in this diagram (the sign is opposite for port). The obtained stroke curves match the results of van Holst's simulation [9] and his reference measurements. The stroke rate is 34 $min^{-1}$ and the average boat velocity is slightly above 4.6 m $s^{-1}$, which are both representative numbers for a lightweight under 23 single sculler at race pace, as the GPS data of the 2015 World Championships final show [15].

### *4.2. Experiment 2*

The wind tunnel experiment has been validated by comparing the obtained data for smooth and rough cylinders with values in literature [2] [3] [4]. The experimental results for smooth cylinders with speedstrips are shown in Fig. 4 for diameters of 32, 40 and 50 mm, compared with data for smooth cylinders without speedstrips. Trendlines and vertical error bars (standard deviations) are shown. Statistical analysis shows that the $C_D$ values deviate less than 5% from the average for more than 92.5% of the measurements for speedstrip equipped cylinders. For $Re < 2 \cdot 10^4$, the measurements deviate more than 5%. This is due to the absolute accuracy of the load cells. Using the relation between energy loss and boat velocity in equation (**??**), it is evaluated that the low accuracy for $Re < 2 \cdot 10^4$ accounts for a relative error in the rowing model output of 1%. The data shows lower $C_D$ values compared to smooth cylinder data and confirms the expectation to find an earlier drag crisis with speedstrips. Furthermore, the data suggests that the drag reduction is dependent on the thickness of the oar shaft in relation to the thickness of the speedstrip. The measurements of cylinders under an angle were performed and the results (not presented) indicated that the $C_D$ values for cylinders with speedstrips under an angle of 30 and 60 degrees are similar or even lower than those for perpendicular cylinders. Nevertheless, to prevent overestimation of the obtained advantage due to the application of speedstrips, the results for perpendicular flow is used to calculate the drag force acting on the oar. The rowing mechanics model needs a $C_D$ value along the whole length of the shaft. Along the shaft length the diameter decreases linearly and for this reason the data for the speedstrips has been interpolated. The data has been ‘normalised’ by multiplying the $C_D$-values of each cylinder with the respective cylinder diameter ($C_D \cdot D$). The $C_D$ value for a specific location on the shaft to apply

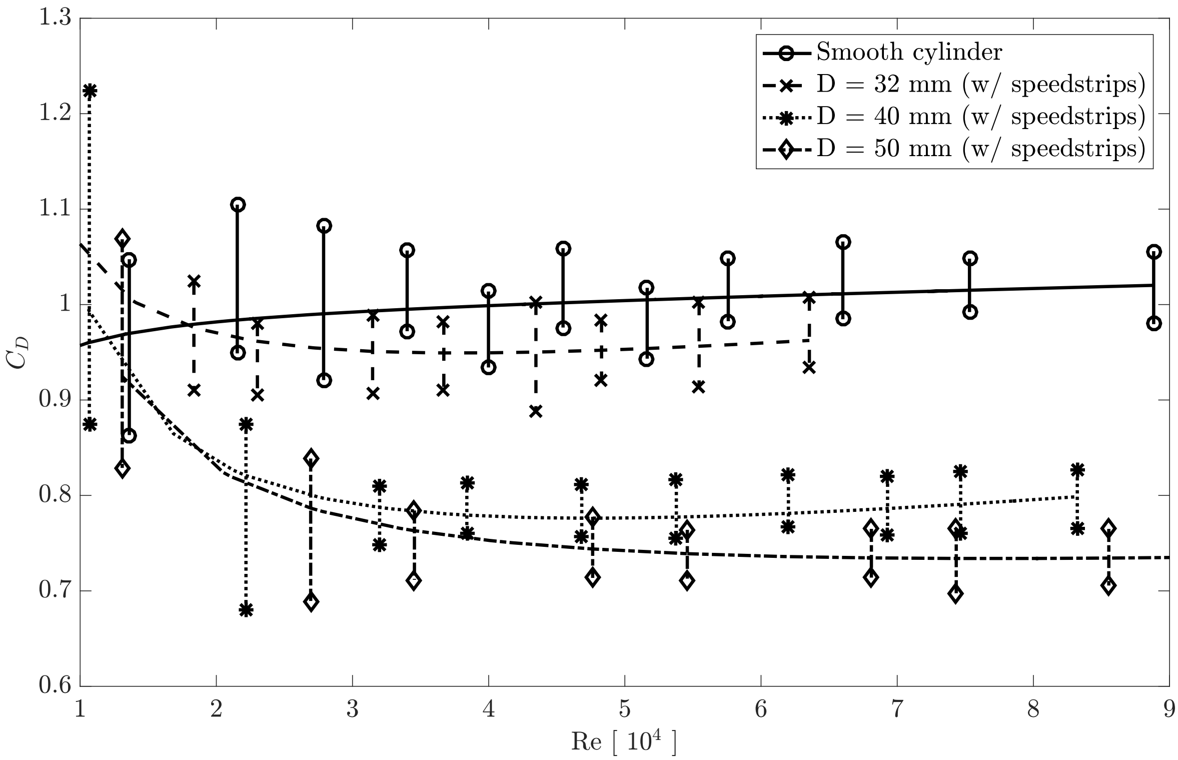


Fig. 4: Experimental results for perpendicular smooth cylinders

in the rowing model is obtained by dividing the ‘normalised’ parameter $C_D \cdot D$ by the diameter of the shaft $D$ at the desired location.

### 4.3. Rowing model

The rowing model has been used to calculate the distance win in a simulated race for a lightweight single sculler equipped with speedstrips on the oars compared to the same boat with smooth oar shafts. The result is a 0.1% advantage for the speedstrip-equipped boat under calm wind conditions, up to 0.4% with a headwind velocity of 5 m s$^{-1}$. The model decomposes the flow velocities over the oars in components ($x$- and $y$-direction) to calculate the resulting forces on the oars, see Fig. 2(b). The results of experiment 2 for oars under an angle show that the longitudinal forces without decomposition could be lower, due to lower $C_D$ values. This suggests that the obtained results of the model are conservative; the advantage could be even larger.

## 5. Conclusions

The goal of this study was to quantify the obtained advantage for a lightweight single sculler by the application of speedstrips on the oar shafts. Experiment 1 has shown that the oars of a single sculler do not encounter Reynolds numbers above $5 \cdot 10^4$ in a race. A rough oar surface would be insufficient to reduce the aerodynamic drag of a rowing oar. Experiment 2 has shown that speedstrips on a cylinder, similar to the size of a rowing oar shaft, induce an earlier drag crisis and reduce the drag in the range of Reynolds numbers encountered in rowing. The rowing model calculations have resulted in a distance win of more than 2 m in calm weather conditions on a 2000 m course, which is equal to a 0.1% advantage. The advantage increases with increasing head wind velocity; for a head wind velocity of 5 m s$^{-1}$, the distance win is more than 8 m (0.4%). The results of experiment 2 show that drag reduction is dependent on the thickness of the oar shaft in relation to the thickness of the speedstrip. More advantage could be achieved if the speedstrip thickness scales with the diameter of the cylinder on which it is being applied. Finding the optimal thickness for a given shaft diameter could be the potential aim of future research on this topic.

## Acknowledgements

The authors express their sincere thanks to L.E. Razoux Schultz for writing the Matlab rowing model, and to S.M. Allebrandi and Z.M.A. Scholten for co-operating the wind tunnel experiment.

## References

[1] Hofmijster, M. J. (2010). Mechanics and energetics of rowing. PhD thesis, Vrije Universiteit, Amsterdam, The Netherlands.
[2] White, F. M. (2003). Fluid mechanics.
[3] Mallick, M., Kumar, A., Tamboli, N., Kulkarni, A. B., Sati, P., Devi, V., & Chandar, S. S. (2014). Study on Drag Coefficient for the Flow Past a Cylinder. International Journal of Civil Engineering Research, 5(4), 301-306.
[4] Kawamura, T., Takami, H., & Kuwahara, K. (1986). Computation of high Reynolds number flow around a circular cylinder with surface roughness. Fluid Dynamics Research, 1(2), 145.
[5] Aoki, K., Muto, K., & Okanaga, H. (2010). Aerodynamic characteristics and flow pattern of a golf ball with rotation. Procedia Engineering, 2(2), 2431-2436.
[6] Choi, J., Jeon, W. P., & Choi, H. (2006). Mechanism of drag reduction by dimples on a sphere. Physics of Fluids (1994-present), 18(4), 041702.
[7] Slangen, R. A. C. M. (2009). Experimental investigation of artificial boundary layer transition. Master of Science Thesis, TU Delft, vol, 82.
[8] Elsinga, G. E., & Westerweel, J. (2012). Tomographic-PIV measurement of the flow around a zigzag boundary layer trip. Experiments in fluids, 52(4), 865-876.
[9] van Holst, M. On rowing `http://home.hccnet.nl/m.holst/RoeiWeb.html` Retrieved: 01-01-2016.
[10] `http://www.knmi.nl/nederland-nu/klimatologie/daggegevens` Retrieved: 01-01-2016.
[11] `http://www.worldrowing.com/athletes/athlete/42157/kuyt-conno` Retrieved: 01-01-2016.
[12] Peach Innovations PowerLine Rowing Instrumentation and Telemetry: `http://www.peachinnovations.com` Retrieved: 01-01-2016.
[13] SCAIME single point load cells, `http://www.scaime.com/en/15/produit/aluminum-single-point-load-cell.html` Retrieved: 01-01-2016.
[14] `http://www.hollandbeker.nl/en/regatta/results/` Retrieved: 01-01-2016.
[15] `http://www.worldrowing.com/assets/pdfs/U23WCH_2015/ROML12101_MGPS.pdf` Retrieved: 01-01-2016.